

## Dynamical theory of x-ray diffraction at Bragg angles near $\pi/2$

Ariel Caticha\* and S. Caticha-Ellis

*Instituto de Física "Gleb Wataghin," Universidade Estadual de Campinas,  
13100 Campinas, São Paulo, Brasil*

(Received 25 February 1981)

The dynamical theory of x-ray diffraction normally makes use of some approximations that, however, cease to be valid when  $\theta_B \simeq \pi/2$ . In this paper we analyze why this happens and establish the theory applicable to this case, obtaining new appropriate expressions the analysis of which allowed us to distinguish three different regimes of diffraction in the neighborhood of  $\pi/2$  (one related to the usual Bragg diffraction, one a transition regime, and a third related to the normal soft-x-ray propagation). The reflectivity of a semi-infinite crystal is then calculated, and extremely large linewidths are found for the rocking curve as compared to the common cases for perfect crystals; the absorption effect on the profiles and the relatively small effect of the orientation of the crystal surface, also studied here, turn out to be quite interesting and may have important practical consequences. As we expected, an extreme sensibility to minute variations of the lattice parameters is found. The peculiar peak shapes and the large linewidths could be of use in high-precision measurements of lattice parameters. Our treatment also provides the theoretical basis for the design of resonant cavities for x rays and other such interferometric devices.

### I. INTRODUCTION

The propagation of electromagnetic radiation in perfect crystals has been object of the attention of many workers in the field of crystal optics both in the case of short (x ray) wavelengths where there are diffracted beams and in the case of longer wavelengths where there is no diffraction. In this work we study the diffraction of x rays in the small spectral region in which there occurs the transition between those two situations and which is characterized by Bragg angles  $\theta_B$  near  $\pi/2$ .

This case has so far received relatively little attention. Exceptions are some general considerations on the dispersion surface in electron diffraction by Stern *et al.*<sup>1</sup> in 1969 and an initial treatment by Kohra and Matsushita<sup>2</sup> in 1972. After the completion of the essential part of this work a paper was published by Brümmer *et al.*<sup>3</sup> dealing with partial aspects in the nonabsorbing case and a proposal for the construction of a Fabry-Pérot-type interferometer for x rays was made by Steyerl and Steinhauser.<sup>4</sup> However, a theoretical study analyzing the phenomena occurring in this peculiar

and yet important limiting situation was still lacking. This paper is an attempt to give a contribution to such a study whose relevance is not restricted merely to its academic interest but may lead to important applications. One example of its possible use is in the development of resonant cavities for x rays in which the radiation is confined in a small region of space by means of successive Bragg reflections by crystal planes oriented perpendicular, or nearly so, to the direction of incidence. Another possible application would be in the development of a new experimental technique for diffraction in the region of extremely high angles where, as is widely known, very high accuracies may be achieved in the measurement of lattice parameters.

Since several of the approximations employed in the usual dynamical theory are not valid when  $\theta_B \simeq \pi/2$ , we will show which expressions cease to be valid and how they should be modified (Sec. II). Overlooking this type of analysis leads to important errors which are probably the main reason for not having a complete theory of these phenomena until now. New expressions, valid in this small angular range, relating the various quantities of phys-

ical interest to the angle of incidence are found (Sec. IV). Then we proceed to their interpretation and perform the calculation of the diffraction profiles and their main parameters for the nonabsorbing (Sec. V) and the absorbing crystal (Sec. VI). Finally, we apply the theory to the diffraction of Co  $K\alpha_1$  by the 620 plane of germanium (Sec. VII) and show how the different cases analyzed below can be obtained, thus changing the shape and the width of the profile, by simply adjusting the temperature of the crystal. This process can be thought of as a means to tune resonant cavities made on this principle. Since some changes in the usual dynamical theory have to be introduced, a very brief preliminary revision of a few important points is in order (Sec. II), so that the origin of these changes may become clear.

## II. THE USUAL FORMULATION OF THE DYNAMICAL THEORY

The formulation of dynamical diffraction theory of von Laue [see e.g., Zachariasen<sup>5</sup> (1945), James<sup>6</sup> (1963), Batterman and Cole<sup>7</sup> (1964), or Kato<sup>8</sup> (1974)] consists of solving Maxwell's equations in a continuous periodic medium. In the two-beam approximation an incident plane wave,

$$\epsilon_0 \vec{E} \exp[-j(\vec{K}_0 \cdot \vec{r} - \nu t)],$$

where  $|\vec{K}_0| = K = \nu/c$  and  $j = 2\pi i$ , excites a Bloch wave within the crystal,

$$e^{j\nu t} (\vec{D}_0 e^{-j\vec{k}_0 \cdot \vec{r}} + \vec{D}_h e^{-j\vec{k}_h \cdot \vec{r}}),$$

where  $\vec{k}_h = \vec{k}_0 + \vec{H}$ ,  $\vec{H}$  being a vector of the reciprocal lattice. In order that the Bloch wave above be a solution of Maxwell's equations satisfying the appropriate boundary conditions, the following must be further imposed.

(a) The wave vectors must lie on the dispersion surface,  $\xi_0 \xi_h = \chi_h \chi_{-h}/4$ , where  $\xi_0$  and  $\xi_h$  are the so-called resonance defects defined by

$$k_0 = k + K\xi_0, \quad k_h = k + K\xi_h, \quad (1)$$

with  $k = K(1 + \chi_0/2)$ , and where  $\chi_h$  is the Fourier component of the dielectric susceptibility corresponding to  $\vec{H}$ .

(b) The amplitude ratio must be

$$R_A \equiv D_h/D_0 = 2\xi_0/\chi_{-h} = \frac{\chi_h}{2\xi_h}. \quad (2)$$

(c) The resonance defect  $\xi_0$  must be given by

$$\xi_0 = \frac{1}{2} [-y \pm (y^2 + b/|b|)^{1/2}] (\chi_h \chi_{-h})^{1/2} |b|^{1/2}, \quad (3)$$

where

$$y = \frac{\chi_0(1-b) + ab}{2|b|^{1/2}(\chi_h \chi_{-h})^{1/2}}, \quad (4)$$

$$b = \frac{\hat{n} \cdot \vec{K}_0}{\hat{n} \cdot (\vec{K}_0 + \vec{H})}, \quad (5)$$

$$a = K^{-2}(2\vec{K}_0 \cdot \vec{H} + H^2), \quad (6)$$

and  $\hat{n}$  is the unit normal to the crystal surface oriented inwards (see Fig. 1).

We are interested in the Bragg case diffraction by a semi-infinite crystal. The directly measurable quantity is the reflectivity  $R_p$  or power ratio:

$$R_p \equiv |R_A|^2 / |b| = |\chi_h/\chi_{-h}| | -y \pm (y^2 - 1)^{1/2} |^2. \quad (7)$$

The important point to be made in repeating such well-known expressions is that nowhere in their deduction does one use the fact that  $\theta_B$  differs appreciably from  $\pi/2$ ; that is, the expressions above are valid irrespective of  $\theta_B$  being near to  $\pi/2$  or not. The approximations so far made are justified by the facts that the susceptibility is a very small quantity ( $10^{-5}$  or  $10^{-6}$ ) and that in order to treat interference phenomena it is necessary to keep good precision only in the calculation of phases (i.e., wave vectors) and not in the calculation of amplitudes. Thus in expressions (1) one

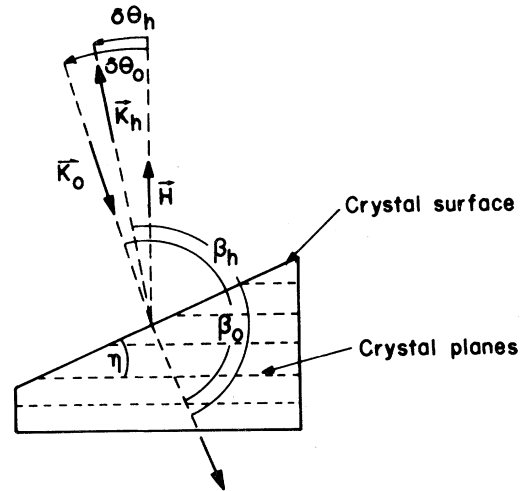


FIG. 1. Various geometrical quantities of interest.

keeps terms of order  $\chi$  [denoted  $O(\chi)$  in what follows] neglecting  $O(\chi^2)$ , while in expressions (2) and (7) dealing with amplitude one keeps only  $O(1)$ .

The quantities of physical interest ( $k_0, k_h, R_A, R_p$ , etc.) are written as functions of the resonance defects which in turn are expressed in terms of the auxiliary variable  $y$  generally defined by (4). It is this last variable that is related to the angle of incidence  $\theta_0$  (the angle between  $\vec{K}_0$  and the crystal planes), for example,  $R_A = R_A(\xi_0(y(\theta_0)))$ . Only in the last step, i.e., in the expression  $y = y(\theta_0)$ , is the condition used that  $\theta_B$  (the kinematical Bragg angle) be near to  $\pi/2$  or not. Thus, in the usual case where  $\theta_B$  differs appreciably from  $\pi/2$  (say  $1^\circ$  or more), the small angular deviation from  $\theta_B$ ,  $\Delta\theta_0 = \theta_B - \theta_0$ , over which there is appreciable diffraction, is of the order  $\chi$  and therefore  $\delta\theta_0^2$  may be safely neglected. Expressions (5) and (6) then take their usual forms:

$$b \simeq \frac{\hat{n} \cdot \vec{K}_0}{\hat{n} \cdot K_h} = \frac{\gamma_0}{\gamma_h} \quad (5')$$

and

$$a = 2\Delta\theta_0 \sin 2\theta_B. \quad (6')$$

By substituting  $a$  from (6') into (4) one obtains a linear relationship between the auxiliary variable  $y$  and the angular variable  $\Delta\theta_0$ :

$$y = |b|^{-1/2} (\chi_h \chi_{-h})^{-1/2} \times \left[ \frac{1}{2} \chi_0 (1-b) + b \Delta\theta_0 \sin 2\theta_B \right]. \quad (8)$$

Equation (8) is valid whenever  $\theta_B \neq \pi/2$ . (The symbol  $\neq$  as used here indicates that the magnitudes related by it are not close enough to warrant the validity of the new approximations set up in this paper.) One can observe in passing that  $y$  does not change if  $H$  is interchanged with  $-H$  even when anomalous dispersion is present. As we shall soon show, the relation between  $y$  and  $\Delta\theta_0$  when  $\theta_B \simeq \pi/2$  is no longer linear but cubic in  $\Delta\theta_0$ , a fact which has far-reaching consequences in the theory developed below. It will be shown that in this case the width of the diffraction peak is of the order  $\chi^{1/2}$ . (This conclusion was first obtained by Kohra and Matsushita<sup>2</sup> in the case of nonabsorbing crystals by means of a geometrical study of the dispersion surface.) Here, this means that  $\Delta\theta_0 \simeq O(\chi^2)$  should not be neglected.

### III. DEFINITIONS AND NOTATION

Let  $\chi'_h$  and  $\chi''_h$  be, respectively, the real and the imaginary parts of  $\chi_h$  and let  $\theta_{\mathcal{B}}$  be the Bragg an-

gle corrected by the average index of refraction:

$$H = 2k_r \sin \theta_{\mathcal{B}}, \quad (9)$$

with  $k_r = K(1 + \chi'_0/2)$ . Let us define the quantity  $\epsilon$  in the region  $\theta_{\mathcal{B}} \simeq \pi/2$ ,

$$H = 2K(1 + \epsilon), \quad (10)$$

where  $\epsilon$  is a small quantity of order  $\chi$ .

It is convenient to measure the angles of incidence and diffraction from the normal to the crystal planes and to take the counterclockwise sense as positive (Fig. 1):  $\delta\theta_0 = \pi/2 - \theta_0$  and  $\delta\theta_h = \pi/2 - \theta_h$ . Finally, let  $\eta$  be the angle between the crystal surface and the diffracting planes and define

$$\tau = \tan \eta. \quad (11)$$

### IV. SOME EXPRESSIONS VALID WHEN $\theta_{\mathcal{B}} \simeq \pi/2$

#### A. Relation between the angles of incidence and diffraction

The condition of tangential continuity of the wave vectors,  $\vec{K}_{ht} - \vec{K}_{0t} = \vec{H}_t$ , may be written in the form (see Fig. 1)

$$K[\sin(\eta - \delta\theta_h) + \sin(\eta - \delta\theta_0)] = H \sin \eta$$

or, using (10) and (11) and keeping terms up to  $O(\chi)$ ,

$$\frac{1}{2} \tau (\delta\theta_0^2 + \delta\theta_h^2) + \delta\theta_0 + \delta\theta_h + 2\epsilon\tau = 0, \quad (12)$$

and solving for  $\delta\theta_0$  or  $\delta\theta_h$  and using the approximation  $(1+x)^{1/2} \simeq 1 + \frac{1}{2}x - \frac{1}{8}x^2$ , one obtains

$$\delta\theta_0 = -\delta\theta_h - \tau\delta\theta_h^2 - 2\epsilon\tau, \quad (13)$$

and a similar expression for  $\delta\theta_h$  with indices 0 and  $h$  interchanged. The second root of (12) is not consistent with the approximations made and therefore lacks physical meaning.

#### B. The asymmetry parameter $b$ and the variables $a$ and $y$

From (5), (6), and (10), using

$$\vec{n} \cdot \vec{K}_0 = -K \cos(\eta - \delta\theta_0)$$

and

$$\vec{H} \cdot \vec{K}_0 = -HK \cos \delta\theta_0,$$

one obtains

$$b = -1 - 2\tau\delta\theta_0 + O(\chi) \quad (14)$$

and

$$a = 2(\delta\theta_0^2 + 2\epsilon) + O(\chi^2). \quad (15)$$

Substituting these into (4) and using the expansion  $(1+x)^{-1/2} = 1 - \frac{1}{2}x + \dots$ , we get

$$y = -(\chi_h \chi_{-h})^{-1/2} \times [\tau \delta \theta_0^3 + \delta \theta_0^2 + 2\epsilon \tau \delta \theta_0 - (\chi_0 - 2\epsilon)] + O(\chi). \tag{16}$$

**C. Incidence and diffraction angles as functions of  $y$**

To obtain  $\delta \theta_0 = \delta \theta_0(y)$  one solves the cubic equation (16) for  $\delta \theta_0$ . The result, correct to  $O(\chi)$ , is

$$\delta \theta_0(y) = \pm [\chi_0 - 2\epsilon - y(\chi_h \chi_{-h})^{1/2}]^{1/2} - \frac{1}{2} \tau [\chi_0 - y(\chi_h \chi_{-h})^{1/2}]. \tag{17}$$

The substitution of (17) into the equivalent of (13) with  $0$  and  $h$  interchanged leads to

$$\delta \theta_h(y) = \mp [\chi_0 - 2\epsilon - y(\chi_h \chi_{-h})^{1/2}]^{1/2} - \frac{1}{2} \tau [\chi_0 - y(\chi_h \chi_{-h})^{1/2}]. \tag{18}$$

The presence of the double signs is easily understood: There are two directions in the same plane of incidence which satisfy the diffraction condition, one corresponding to  $\theta_{\mathcal{D}}$  and the other to  $\pi - \theta_{\mathcal{D}}$ . The third root of (16) lacks physical meaning since it is of the order of  $1/\tau$  or about

$O(1)$  and does not correspond to the case  $\theta_{\mathcal{D}} \simeq \pi/2$ . The symmetry between (17) and (18) together with the fact that the reflectivity given by (7) is only a function of  $y$  implies the applicability of Helmholtz's reciprocity theorem to x-ray dynamical diffraction with or without absorption when  $\theta_{\mathcal{D}} \simeq \pi/2$ .

**V. THE DIFFRACTION PROFILE WITHOUT ABSORPTION**

The diffraction profile is obtained by substituting (16) into (7):  $R_p = R_p[y(\delta \theta_0)]$ . (Here we disagree with Kohra and Matsushita.<sup>2</sup> They claim that intensities are obtained by the replacement of  $y$  by  $y^2$ , which does not seem to be the case.) Let  $(\chi_h \chi_{-h})^{1/2} = |\chi_h|$  and  $\chi_0 = \chi'_0$ , then  $y$  is real.

**A. Three Cases**

We shall pay attention solely to the region of total reflectivity (RTR) in which  $|y| < 1$  leads to  $R_p = 1$ . The limits of the RTR are easily obtained by substituting  $y = \pm 1$  into (17):

$$\delta \theta_0^{(\pm)}(\pm 1) = \pm (\chi'_0 - 2\epsilon \mp |\chi_h|)^{1/2} - \frac{1}{2} \tau (\chi'_0 \mp |\chi_h|). \tag{19}$$

The number of real values of  $\delta \theta_0^{(\pm)}(\pm 1)$  allows one to distinguish three cases (Fig. 2).

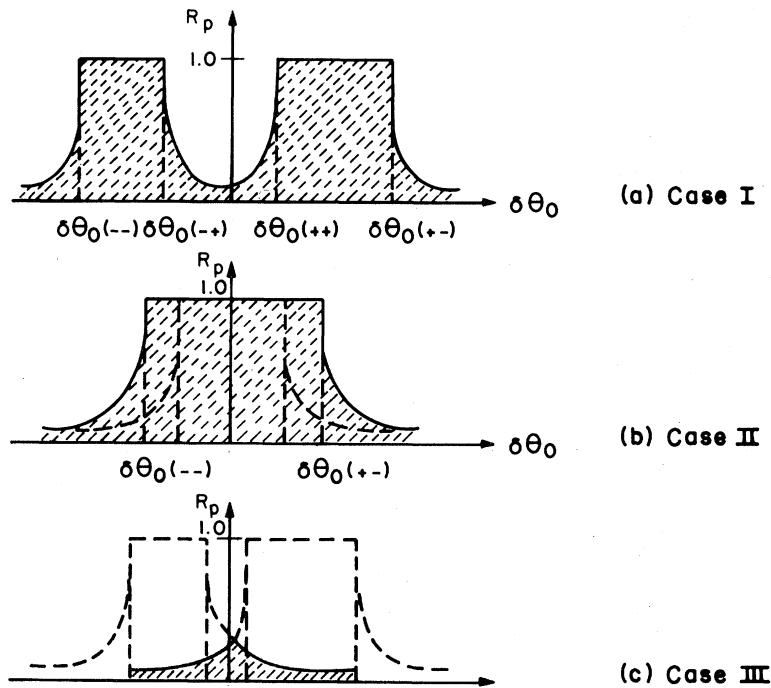


FIG. 2. Diffraction profiles without absorption for  $\theta_{\mathcal{D}} \simeq \pi/2$ .

*Case I:*  $\chi'_0 - 2\epsilon > |\chi_h|$ . There are four real values  $\delta\theta_0^{(\pm)}(\pm 1)$ , i.e., two RTR's.

*Case II:*  $-|\chi_h| < \chi'_0 - 2\epsilon < |\chi_h|$ . There are only two real values  $\delta\theta_0^{(\pm)}(-1)$ , i.e., only one RTR.

*Case III:*  $\chi'_0 - 2\epsilon < -|\chi_h|$ . There is no RTR though there may still be some diffracted intensity.

**B. Linewidths**

We define the width of the diffraction profile as the width of the RTR since this is a useful concept even in the presence of some absorption. From (19); for case I,

$$W_I^{(\pm)} = (\chi'_0 - 2\epsilon + |\chi_h|)^{1/2} - (\chi'_0 - 2\epsilon - |\chi_h|)^{1/2} \mp \tau |\chi_h| \quad (20)$$

$W_I^{(\pm)}$  correspond to  $\delta\theta_0 \gtrless 0$ , respectively, and the linewidth is of  $O(\chi)$ . For case II,

$$W_{II} = 2(\chi'_0 - 2\epsilon + |\chi_h|)^{1/2} \quad (21)$$

Note that in this case the linewidths are of  $O(\chi^{1/2})$ , i.e., from 2 to 3 orders of magnitude larger than those in case I or in the common case  $\theta_{\mathcal{B}} \neq \pi/2$ , so that the approximations used in the previous calculations were made accordingly. In the particular case  $\theta_{\mathcal{B}} = \pi/2$ , one has  $\chi'_0 - 2\epsilon = 0$ , obtaining:

$$W_{II}(\theta_B = \pi/2) = 2|\chi_h|^{1/2} \quad (22)$$

Formula (22), as well as the distinction of the three

different cases, are results first obtained by Kohra and Matsushita<sup>2</sup> by means of a geometrical study of the dispersion surface for nonabsorbing crystals that appear quite naturally in the present general formulation.

**C. Influence of the orientation of the crystal surface**

From (19), the effect of a nonzero  $\tau$  is to shift the limits of the RTR corresponding to  $y = \pm 1$ , respectively, by angles  $\zeta_+$  and  $\zeta_-$  (Fig. 3), given by

$$\zeta_{\pm} = (|\chi'_0| \pm |\chi_h|)\tau/2 \quad (23)$$

In case I one sees a deformation (for  $\zeta_+ > \zeta_- > 0$  when  $\tau > 0$ ) and a displacement of the peak similar to the well-known analogous effect found in the usual dynamical theory. In case II, however, the situation is quite different, since according to Eq. (21)  $W_{II}$  does not depend on  $\tau$ ; the profile is merely shifted as a whole. One should note that while the shifts  $\zeta_{\pm} \sim O(\chi)$  are very important when  $\theta_{\mathcal{B}}$  is not near to  $\pi/2$ , for then the linewidths are also of  $O(\chi)$ . When  $\theta_{\mathcal{B}} \simeq \pi/2$ , one has  $\zeta_{\pm} \ll W$ , which means that the diffraction profile is quite insensitive to the surface orientation. In some applications, however (e.g., an x-ray resonator), this small relative effect might still be of importance. In such cases one may wish to determine the direction of incidence for which the beam will be reflected upon itself. The condition for this to happen is  $\delta\theta_0(\bar{y})$

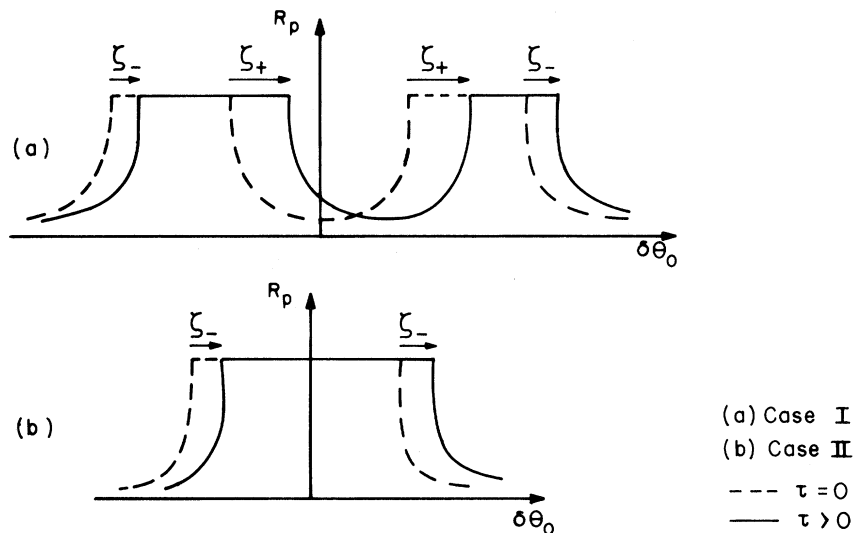


FIG. 3. Effect on the profile of a tilted crystal surface. Not drawn to scale. ---  $\tau=0$ , —  $\tau > 0$ .

$=\delta\theta_h(\bar{y})$ , which from (17) and (18) implies

$$\bar{y}=(\chi_h\chi_{-h})^{-1/2}(\chi_0-2\epsilon), \quad (24)$$

which corresponds to

$$\delta\theta_0(\bar{y})=-\tau\epsilon, \quad (25)$$

a result valid regardless of there being absorption or not.

**D. On the possibility of diffraction occurring at a “complex Bragg angle”**

From (10) and the definition (9) of  $\theta_{\mathcal{B}}$ ,

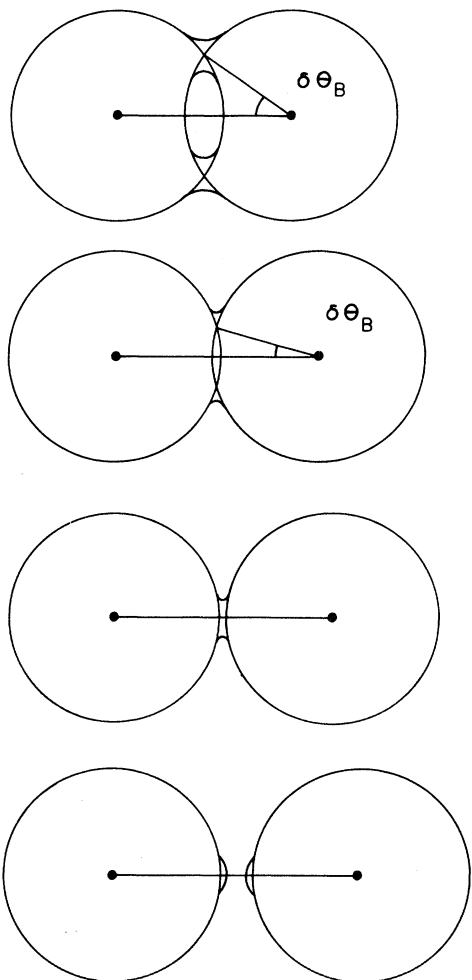
$$\delta\theta_{\mathcal{B}}\equiv\pi/2-\theta_{\mathcal{B}}=\pm(\chi'_0-2\epsilon)^{1/2}. \quad (26)$$

The three cases of Sec. V A may be distinguished according to the value of  $\delta\theta_{\mathcal{B}}^2$  relative to  $|\chi_h|$ ,

there arising the possibility of  $\delta\theta_{\mathcal{B}}$  taking imaginary values. The fact of  $\theta_{\mathcal{B}}$  being complex is interpreted geometrically as the case where the spheres of radius  $k_r$  centered at the reciprocal-lattice points 0 and  $H$  do not intercept each other [Figs. 4(c) and 4(d)]. Even if  $\theta_{\mathcal{B}}$  is complex the diffracted intensity may still be rather high [Fig. 4(c)].

**VI. THE DIFFRACTION PROFILE WITH ABSORPTION**

A very elegant method to study the reflectivity  $R_p=R_p(y(\theta_0))$  in the usual Bragg diffraction case has been proposed by Fingerland.<sup>9</sup> Here, we develop this method further so that with some modifications it may be applied to the case  $\theta_{\mathcal{B}}\simeq\pi/2$ . To do so we write (7) in Miller’s form,<sup>10</sup>



(a) Case I :  $\delta\theta_{\mathcal{B}}^2 > |\chi_h|$

$\delta\theta_{\mathcal{B}}$  real

(b) Case II :  $0 < \delta\theta_{\mathcal{B}}^2 < |\chi_h|$

$\delta\theta_{\mathcal{B}}$  real

(c) Case II :  $-|\chi_h| < \delta\theta_{\mathcal{B}}^2 < 0$

$\delta\theta_{\mathcal{B}}$  imaginary

(d) Case III :  $\delta\theta_{\mathcal{B}}^2 < -|\chi_h|$

$\delta\theta_{\mathcal{B}}$  imaginary

FIG. 4. Dispersion surface when  $\theta_{\mathcal{B}}\simeq\pi/2$ . In (a) and (b)  $\delta\theta_{\mathcal{B}}$  is real while in (c) and (d) it is imaginary.

$$R_p = |\chi_h / \chi_{-h}| [L - (L^2 - 1)^{1/2}], \quad (7')$$

which has the advantage of eliminating the double sign appearing in (7). Here

$$L = |y|^2 + |y^2 - 1|. \quad (27)$$

The study is then performed in three steps as follows.

(a) We construct, following Fingerland, the surface

$$Z(y) = L - (L^2 - 1)^{1/2} \quad (28)$$

in the three-dimensional real space  $(y_i, y_r, Z)$  where  $y = y_r + iy_i$ . Figure 5 gives a representation of such a surface, which we propose to call Fingerland's surface since it is "general and independent of the actual physical situation"<sup>9</sup>; it is, in fact, the same for any Bragg case diffraction by a semi-infinite crystal. Fingerland's study<sup>9</sup> is entirely applicable and need not be repeated here.

(b) Starting from the linear relationship between  $y$  and  $\delta\theta_0$  (which he denoted  $\eta$  and  $\psi$ , respectively), Fingerland showed in the common case  $\theta_{\mathcal{B}} \neq \pi/2$  that there exists a linear relationship between  $y_r$  and  $y_i$  [his equation (9)], so that the profile in the  $y_r$  scale, times  $|\chi_{-h}/\chi_h|$ , is given by the projection on the plane  $(y_r, Z)$  of the intersection of the plane  $y_i = My_r + N$  with Fingerland's surface (Fig. 6). In our case, however, the relationship between  $y$  and  $\delta\theta_0$  is not linear but cubic [Eq. (16)]; we write it in the form

$$y = \alpha f(\delta\theta_0) + \beta, \quad (29)$$

where

$$f(\delta\theta_0) = \tau\delta\theta_0^3 + \delta\theta_0^2 + 2\tau\epsilon\delta\theta_0 - (\chi'_0 - 2\epsilon) \quad (30)$$

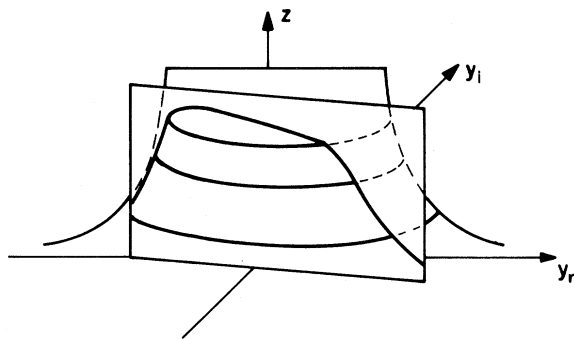


FIG. 5. Sketch of Fingerland's surface  $Z(y) = L - (L^2 - 1)^{1/2}$  and its interception with the plane:  $y_i = My_r + N$ .

is a real function, while

$$\alpha = \alpha' + i\alpha'' = -(\chi_h \chi_{-h})^{-1/2}, \quad (31)$$

$$\beta = \beta' + i\beta'' = -\alpha\chi'_0$$

are complex constants.

Using the same procedure, i.e., separating  $y$  into real and imaginary parts and eliminating  $f(\delta\theta_0)$ , we get the same linear relationship between  $y_r$  and  $y_i$  with

$$M = \alpha''/\alpha', \quad N = -\chi''_0 |\alpha|^2/\alpha'. \quad (32)$$

It is to be noted that all dependence on  $\tau$  has disappeared: The profile on the  $y_r$  scale is independent of the crystal surface orientation.

(c) Transforming from  $y_r$  to  $\theta_0$  we obtain the desired profile. In the usual approximation this is a trivial step since because of the linear relation between  $y$  and  $\theta_0$  this involves just a change of both scale and origin. However, when  $\theta_{\mathcal{B}} \simeq \pi/2$  the situation is more complicated. From (29), (30), and (31):

$$y_r = \alpha' [\tau\delta\theta_0^3 + \delta\theta_0^2 + 2\tau\epsilon\delta\theta_0 - (\chi'_0 - 2\epsilon)] + \chi''_0 \alpha'' \quad (33)$$

The most interesting feature of curve  $y_r = y_r(\delta\theta_0)$  is that  $y_r$  attains a local maximum for  $\delta\theta_0 = -\tau\epsilon$  [this corresponds to  $y = \bar{y}$  given by (24) which is in the region where appreciable diffraction occurs]. The three cases I, II, and III may again be distinguished according to whether  $\bar{y}_r \gtrsim 1$ ,  $|\bar{y}_r| \lesssim 1$ , or  $\bar{y}_r \lesssim -1$ , respectively (Fig. 7). Owing to absorption the transition from one to another case occurs gradually.

If we study Figs. 6 and 7 simultaneously, the qualitative features of the profile may be obtained. The process of generating these profiles is graphically illustrated in Fig. 8. To the left there appears the section of Fingerland's surface; when  $\delta\theta_0$  varies, this section is followed up to the maximum  $\bar{y}_r$  of  $y_r$  and then back again following the descent of the curve  $y_r = y_r(\delta\theta_0)$ . The profile thus generated appears on the right of the same figure. It is obvious that in the normal case  $\theta_{\mathcal{B}} \simeq \pi/2$ , since the relationship  $y = y(\delta\theta_0)$  is linear, the section of Fingerland's surface is passed over just once in a given direction. In our case this "walk" back and forth on Fingerland's surface is indicated schematically by a curved arrow below the figure. For instance, in case I [Figs. 7(a), 8(a), and 9(a)], as  $\delta\theta_0$  increases  $y_r$  enters the region of high reflectivity (RHR) producing a peak similar to that of Fig. 6,

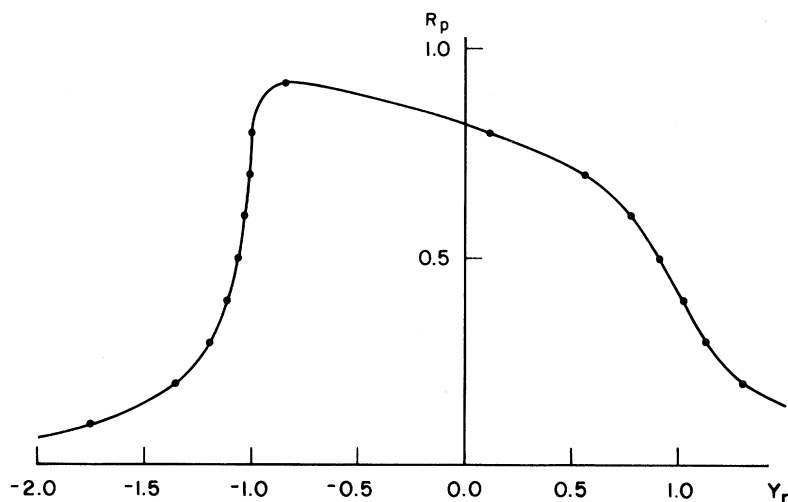


FIG. 6. Diffraction profile in the  $y_r$  scale.

$y_r$  then becomes greater than unity, and  $R_p$  drops to nearly zero. A further increase in  $\delta\theta_0$  makes  $y_r$  retrace its steps back into the RHR producing another peak, almost a mirror reflection of the first (such profiles calculated in a particular case in Sec. VII are shown in Fig. 9). In case II [Figs. 7(b), 7(c), and 8(b)] the situation is quite similar except that  $y_r$  enters the RHR and starts its return before a large drop of  $R_p$  occurs. The asymmetry of  $R_p(y_r)$  will appear in  $R_p(\delta\theta_0)$  as a small dip in the center of the profile. In some applications it may be convenient to eliminate it by choosing the experimental conditions so that the return value  $\bar{y}_r$  occurs at the point where  $R_p(y_r)$  becomes maximum [Fig. 8(c)]. In case III  $y_r$  never enters the RHR but there may still be a small diffraction peak [Figs. 7(d), 8(d), and 9(f)].

In all three cases the effect of the orientation of the crystal surface (which is always small) is taken into account through the asymmetry of the curve (33). For a symmetrical ( $\tau=0$ ) geometry (33) becomes a parabola and the profiles are even functions of  $\delta\theta_0$ .

#### VII. APPLICATION TO THE DIFFRACTION OF $\text{Co } K\alpha_1$ BY $\text{Ge } (620)$

We apply the two-beam theory developed above to the specific example of the diffraction of  $\text{Co } K\alpha_1$  radiation by the 620 planes of germanium. This choice was motivated by the actual feasibility of the experiment (cobalt x-ray tubes and perfect

germanium crystals are easily available) but it suffers from a problem. When  $\theta_{\text{B}}$  and  $\delta\theta_0$  differ from  $\pi/2$  and 0, respectively, by less than  $O(\chi)$ , due to the high symmetry of the cubic lattice one deals, not with a two-beam case but with a 24-beam case. Luckily, this should not be a serious practical drawback because the dynamical multiple beam resonance region is very small (some seconds of arc) compared to the two-beam resonance region (about ten minutes of arc). Anyway, all considerations made below are of general applicability and are not restricted to this special situation of  $\text{Co } K\alpha_1$  and  $\text{Ge } 620$ .

The structure factors were calculated by using data from Ref. 11:  $F(000)=249.12+i9.36$  and  $F(620)=111.12+i9.36$ . Temperature corrections were taken into account through a coefficient of thermal expansion of  $6 \times 10^{-6} \text{ }^\circ\text{C}^{-1}$  and through a Debye-Waller factor  $e^{-M}=0.84$  calculated for  $T=11^\circ\text{C}$  using a Debye temperature of 290 K. The factor  $e^{-M}$  may be considered practically constant in the range  $5-15^\circ\text{C}$ . Very accurate values for both the wavelength and the lattice parameter are needed:  $\lambda=1.788\,965 \text{ \AA}$  (Ref. 11) and  $a=5.657\,820$  at  $25^\circ\text{C}$  [Hom, Kiszénick, and Post (Ref. 12)]. Some numerical results and the profiles are shown in Table I and Fig. 9, respectively. One should note the following:

- The large linewidths and integrated intensities.
- The decrease of linewidths as the temperature increases and the situation approaches that of the usual theory.

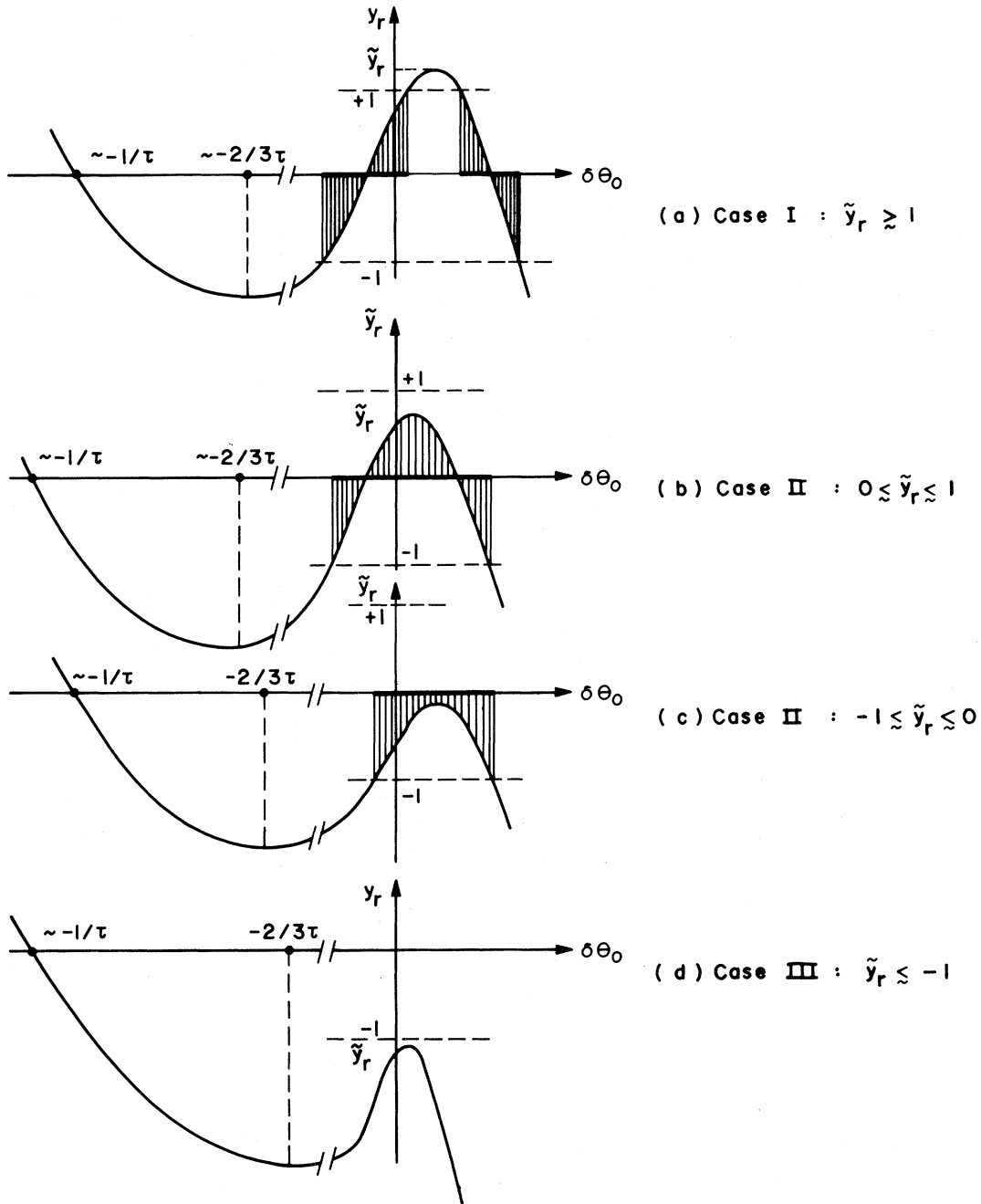


FIG. 7. Transformation  $y_r = y_r(\theta_0)$  when  $\theta_{\mathcal{B}} \simeq \pi/2$ . Not drawn to scale.

(c) The asymmetry of the peaks in case I is a feature which should not be difficult to observe when  $\theta_{\mathcal{B}} \simeq \pi/2$ .

(d) The central dip in case II, which obviously has the same well-known physical origin as the asymmetry of (c).

(e) The peculiar "square" shape obtained when the central dip is eliminated [Fig. 9(e)] is explained by the action of the stationary point in (33) which abnormally "stretches" the region around which  $R_p$  is maximum.

(f) The rapid decrease in  $R_p$  in case III.

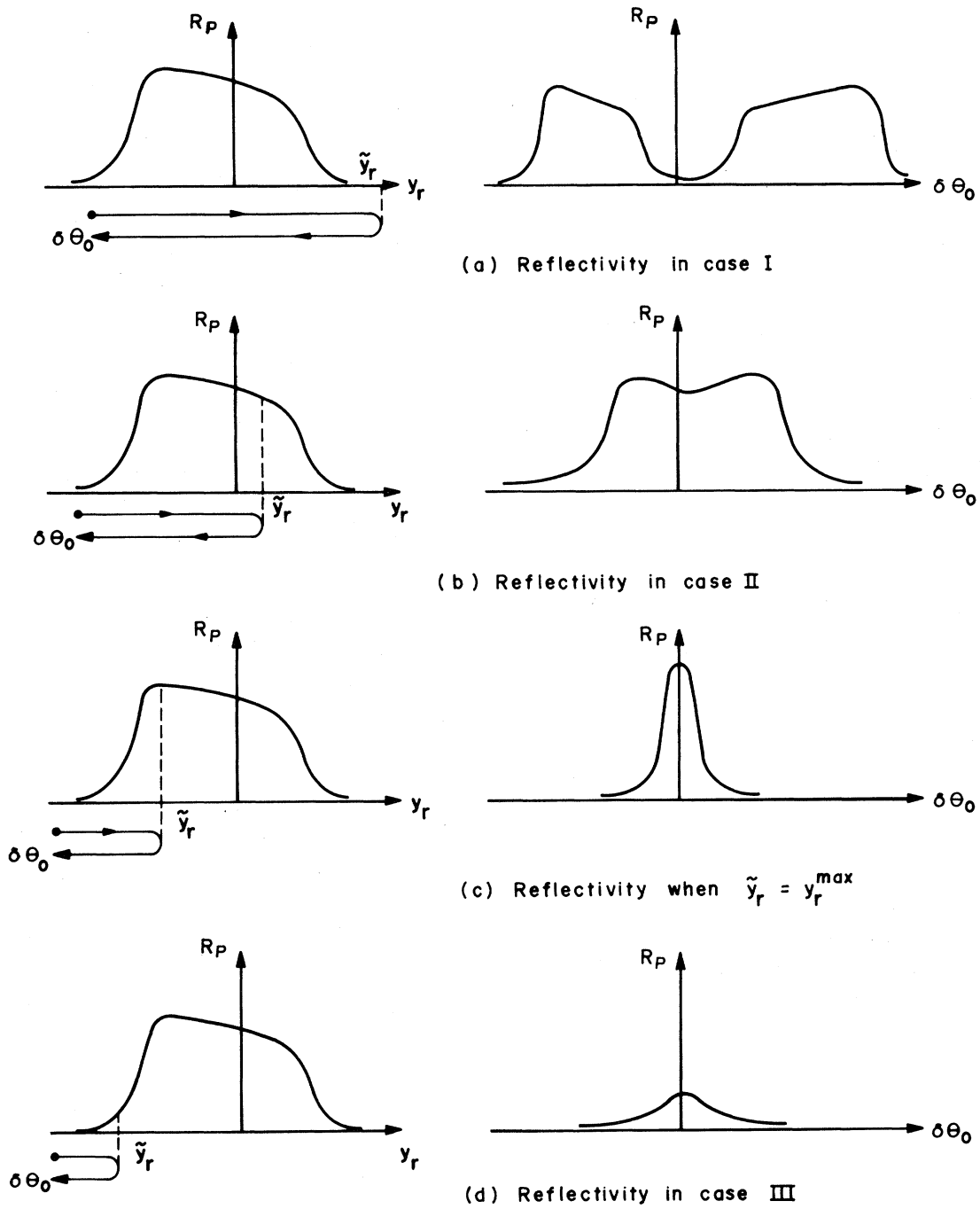


FIG. 8. Illustrating the mathematical process of generating the profile  $R_p = R_p(y(\theta_0))$  described in the text.

(g) The high sensibility of the profiles to the value of the lattice parameter. This implies that the actual profile may depend upon the particular sample used.

(h) Multiple beam effects modify the profile 9(d), but they do so in a region about  $\delta\theta_0=0$  which is so narrow that it does not appear in the scale of the figures.

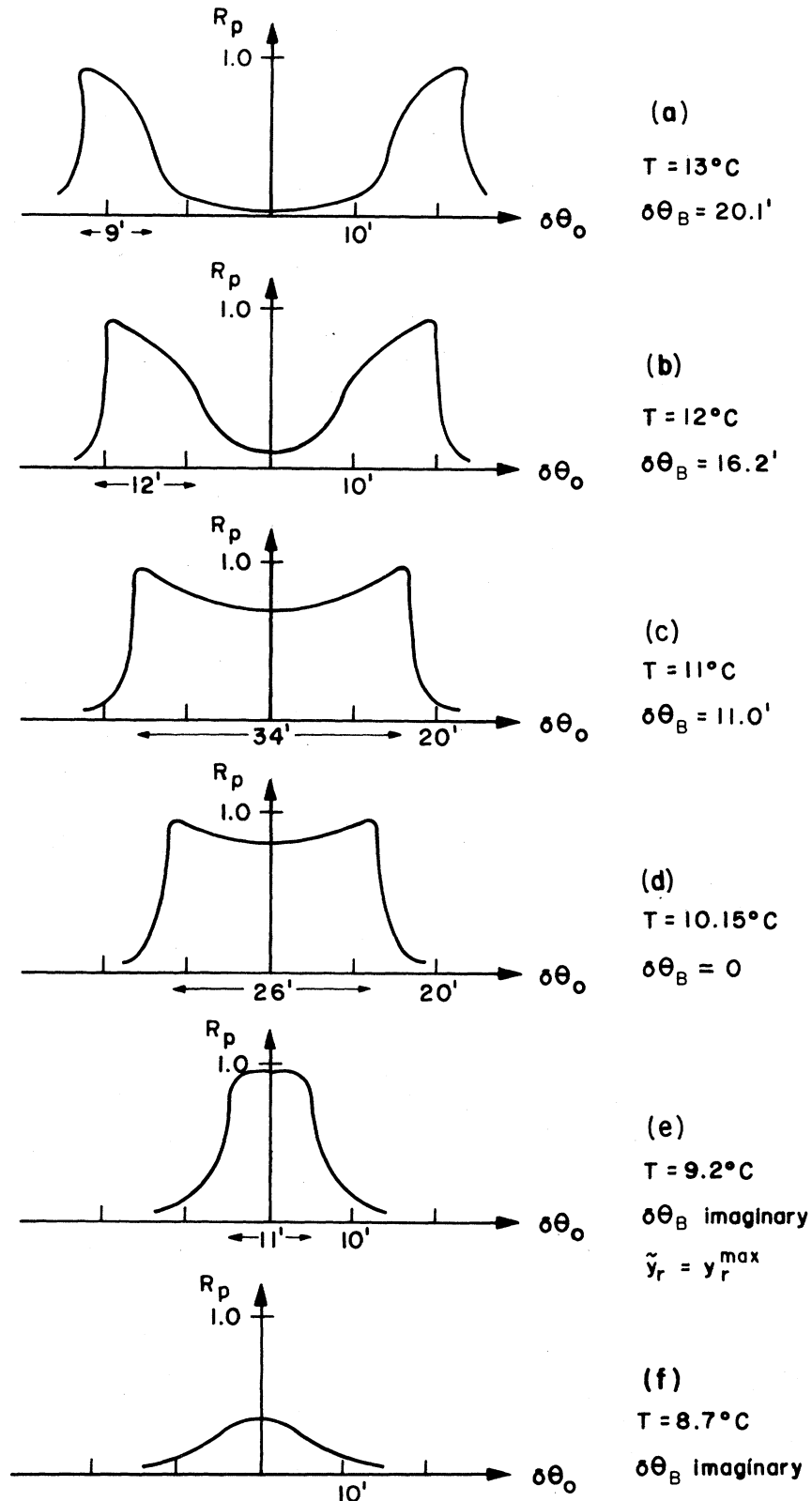


FIG. 9. Calculated diffraction profiles of Ge (620) using  $\text{CoK}\alpha_1$  radiation at various temperatures,  $\theta_{\text{B}} \simeq \pi/2$ ,  $\tau=0$ . Information about these profiles is given in Table I.

TABLE I. Information concerning the profiles of Fig. 9.

Profile	(a)	(b)	(c)	(d)	(e)	(f)
$T$ ( $^{\circ}\text{C}$ )	13.0	12.0	11.0	10.15	9.2	8.7
$\delta\theta_B$ (min)	20.1	16.2	11.0	$\simeq 0$	imag.	imag.
Linewidth (min)	9	12	34	26	11	
Case	I	I	II	II	II	III

### VIII. CONCLUSIONS

The key point in solving the dynamical diffraction problem when  $\theta_{\mathcal{B}} \simeq \pi/2$  lies in writing the reflectivity as  $R_p = R_p(y)$  with  $y = y(\theta_0)$  and noticing that due to the convenient choice of  $y$  the form of  $R_p(y)$  is independent of  $\theta_B$ , so that one has only to modify  $y(\theta_0)$ . Even though applied here only to a semi-infinite crystal the method may be used for finite crystals: One would use the curve  $R_p' = R_p'(y)$  appropriate for finite crystals given by the usual theory combined with  $y_r = y_r(\theta_0)$  given by (33).

After explaining the approximations appropriate for  $\theta_{\mathcal{B}} \simeq \pi/2$  we obtained expressions for the various quantities of physical interest the analysis of which led to the distinction of three cases. Case I is a limiting situation of the usual dynamical theory, while the normal soft x-ray propagation is the asymptotic situation of our case III. The transition region or case II exhibits peculiarities of its own. We obtained expressions for the large linewidths (several minutes of arc), studied the very small effect (shifts of seconds of arc) of the orientation of the crystal surface, called attention to the possibility of there being rather intense diffracted intensity under conditions of a complex Bragg angle, and studied the effect of absorption on the profiles, noticing that in case II the peak exhibits a cu-

rious central depletion.

We would like to point out that the extreme sensibility of the diffraction profiles to the lattice parameter and the large linewidths suggest the possibility of the development of a new diffraction technique with  $\theta_{\mathcal{B}} \simeq \pi/2$  for various precision measurements and studies of crystal imperfections. Actually, one may think of the transformation (33) with a stationary point in the region of intense diffraction acting as a lens magnifying all the details of the curve  $R_p = R_p(y)$ . Finally, we note that the approximations developed in this paper constitute the theoretical basis necessary for the design of resonant cavities for x rays and various other such interferometric devices. Experimental work aimed at the verification of some of the theoretical conclusions arrived at in this paper is now being performed in this laboratory and will be reported in a near future.

### ACKNOWLEDGMENTS

One of us (A.C.) acknowledges a fellowship from FAPESP (Fundo de Amparo à Pesquisa do Estado de São Paulo). Grant No. 2222.1785/78 from CNPq (Conselho Nacional de Desenvolvimento Técnico-Científico) is also gratefully acknowledged.

\*Present address: California Institute of Technology, Physics Department, Pasadena, CA 91125.

<sup>1</sup>R. M. Stern, J. J. Perry and D. S. Boudreau, *Rev. Mod. Phys.* **41**, 275 (1969).

<sup>2</sup>K. Kohra and T. Matsushita, *Z. Naturforsch.* **27a**, 484 (1972).

<sup>3</sup>O. Brümmer, H. R. Höche, and J. Nieber, *Phys. Status Solidi A* **53**, 565 (1979).

<sup>4</sup>A. Steyerl and K. A. Steinhauser, *Z. Phys. B* **34**, 221

(1979).

<sup>5</sup>W. H. Zachariasen, *Theory of X-Ray Diffraction in Crystals* (Wiley, New York, 1945).

<sup>6</sup>R. W. James, in *Solid State Physics*, edited by F. Seitz, H. Ehrenreich, and D. Turnbull (Academic, New York, 1963), Vol. 15, p. 55.

<sup>7</sup>B. Batterman and H. Cole, *Rev. Mod. Phys.* **36**, 681 (1964).

<sup>8</sup>N. Kato, in *X-Ray Diffraction*, edited by L. Azároff

(McGraw-Hill, New York, 1974), Chap. 4.

<sup>9</sup>A. Fingerland, *Acta Crystallogr. A* 27, 280 (1971).

<sup>10</sup>F. Miller, *Phys. Rev.* 47, 209 (1935).

<sup>11</sup>*International Tables for X-Ray Crystallography*

(Kynoch, Birmingham, 1968), Vol. III.

<sup>12</sup>T. Hom, B. Kiszénick, and B. Post, *J. Appl. Crystallogr.* 8, 457 (1975).